High-quality optical modes in low-dimensional arrays of nanoparticles: application to random lasers

A. L. Burin

Department of Chemistry and Department of Physics and Astronomy, Northwestern University, Evanston, Illinois 60208-3113, and Department of Chemistry, Tulane University, New Orleans, Louisiana 70118

H. Cao

Department of Physics and Astronomy, Northwestern University, Evanston, Illinois 60208-3113

G. C. Schatz and M. A. Ratner

Department of Chemistry, Northwestern University, Evanston, Illinois 60208-3113

Received April 7, 2003; revised manuscript received July 28, 2003; accepted August 1, 2003

The optical modes in finite partially ordered arrays of dielectric particles are studied within the coupled dipole approach. It is shown that high-quality modes can be attained under conditions of small enough interparticle distance when the light-cone constraint is satisfied. We performed analytical and numerical investigations of these modes to determine their dependence on system size, dimensionality, and extent of disordering. The opportunity to use these modes to make high-performance random lasers is discussed. © 2004 Optical Society of America

OCIS codes: 140.0140, 050.1670, 160.2900.

1. INTRODUCTION

Recent development in nanoscience makes it possible to design arrays of dielectric or metal particles whose sizes are comparable to or less than the wavelength of light. Under these conditions light interference becomes extremely strong, leading to phenomena previously known only for electrons, including the forbidden optical band in photonic crystals,[1,2] strong localization of light,[3,4] surface enhancement of scattering,[5] and optical nonlinearity[6–9] in hot spots formed by quasi-localized plasmon waves[10,11] and mirrorless microsized lasers.[12–14]

An external electromagnetic field induces oscillations of the polarization within a single metal or dielectric particle. In a metal particle these oscillations are due to the motion of conduction electrons, whereas in a dielectric particle they are associated with the virtual excitation of electron–hole pairs. In both cases the relationship between wavelength and particle size leads to resonances that are plasmon resonances in metals and Mie resonances in dielectrics. Usually plasmon resonances are narrow compared with the resonant frequency, whereas Mie resonances get narrow for sufficiently large dielectric constants. When particles form an array, resonance oscillations in different particles are coupled by electromagnetic interaction. This coupling can form collective polariton modes, which are Mie polaritons in dielectrics and plasmon polaritons in metals. When resonance width and coupling are smaller than the resonant frequency, collective polaritons are formed in the same qualitative manner in metals and dielectrics, so we use the word "polariton" to describe collective modes in both cases.

It is recognized both theoretically and experimentally[15–23] that photonic crystals, composed of ordered arrays of identical nanoparticles, can contain polariton modes of high quality as the result of formation of an optical bandgap. Even in the case of an incomplete bandgap that exists in certain directions only, optical modes near the band edge have long lifetimes because of their small group velocity.[18,19] Systems with complete photonic bandgaps and relatively small disordering should show Anderson localization of light near the band edges. The localized modes[24] possess an extremely high quality factor that grows exponentially with system size.[25]

These high-quality modes in disordered and partially ordered structures can be significant for the performance of random lasers.[12–14,25,26] Random lasing starts when the gain caused by external pumping exceeds the loss for at least one mode that has the longest lifetime.[27–29] Accordingly, the lasing threshold, defined as the minimum gain rate needed to reach lasing, should be small for high-quality modes of interest. The most efficient lasing can be expected from three-dimensional (3-D) structures pumped deeply inside.

From a practical perspective, it is hard to pump a real sample much deeper than a few surface layers because of strong absorption at the pumping frequency [for example, in ZnO powder the absorption length of pump light from a Nd:YAG laser is of the order of 1 μm (Ref. 29)]. It is also

0740-3224/2004/010121-11$15.00

difficult to produce highly ordered 3-D arrays. The problem can be simplified if one is dealing with lower-dimensional structures, including two-dimensional (2-D) planar layers and one-dimensional (1-D) chains of particles placed at the substrate surface. We refer to these structures as open systems[28] because they do not have a bulk part (see Fig. 3 below) and are strongly coupled to the external (vacuum) photons everywhere (in contrast to 3-D systems coupled to the outside reservoir through a surface of zero measure compared to the bulk).

Under certain conditions regular open structures can have long-living guided polariton modes caused by the light-cone constraint[22,23,30] that prevents emission of photons by polaritons with simultaneous conservation of energy and momentum. These guided modes should possess an infinite quality factor in an infinitely large ordered system and a finite but high quality factor Q in large and weakly disordered systems. Note that these modes are more interesting for dielectric scattering particles than for metal ones because absorption in metals by the conduction electrons strongly reduces mode quality.[10,31] Excitation of these modes can be performed most efficiently in the fluorescence regime (accompanied by an internal conversion of optical energy). Use of direct excitation to generate hot spots in clusters of metal particles[10] is difficult, because these modes are dark in emission,[31] i.e., weakly coupled to the external electromagnetic field.

In this paper we study the quality of these modes and their dependence on system size, disordering, and dimensionality, using both analytical and numerical approaches. In Section 2 we formulate the light-cone criterion for the appearance of guided modes in a chain and in a planar layer of ordered particles. Section 3 contains an analytical study of the mode decay rates in infinite chains and their size dependence for finite systems. In Section 4 we report the results of numerical investigations of mode quality in the coupled-dipole approach[6] for finite, partially ordered, low-dimensional arrays. In Section 5 the implications for random lasing are discussed and conclusions are formulated.

2. LIGHT-CONE CONDITIONS

The light-cone constraint is concerned with the momentum-conservation law for the decay of a polariton by photon emission. Assume that we have an infinite 1-D or 2-D regular array of particles located in vacuum. If this array has translational invariance in a certain direction, the projection of the quasi-momentum of the polariton onto the respective axis is conserved. Then excitation of the medium with quasi-momentum k along the translational invariant direction can lead to emission of a photon with a different momentum q, defined by the photon dispersion law, only along the light cone (Fig. 1). If the quasi-momentum of excitation k exceeds photon momentum q, the light cone vanishes and photon emission becomes impossible.

For illustration, consider a 1-D chain of identical particles (Fig. 2) that have resonant frequency ω_0, caused by an internal resonance (which can be a Mie resonance in dielectric particles or a plasmon resonance in metal particles). We assume that this resonance is narrow, such that its width is smaller than ω_0. Then we can ignore the dispersion of polariton waves in the medium. This assumption is normally satisfied for plasmon resonances, whereas for Mie resonances it requires the dielectric constant of the particles to be much greater than 1. However, we do not expect qualitative changes in mode quality if dispersion is taken into account carefully. Let the interparticle distance be a and the particle diameter be d.

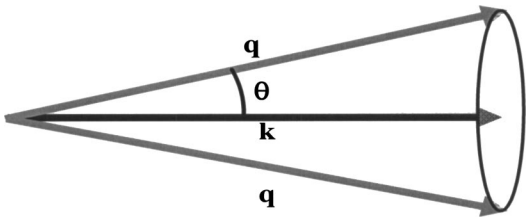

Fig. 1. Emission of light from the 1-D chain excitations along the cone surface defined by the condition $q\cos(\theta) = k$, where q is the momentum of the emitted photon and k is the momentum of the excitation (see text for details). When $k > q$ one gets $\cos(\theta) > 1$, and light emission becomes impossible because of the light-cone constraint.

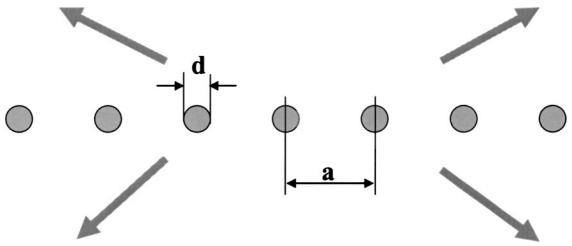

Fig. 2. 1-D chain of resonant spherical particles (diameter d) with period a. Arrows, directions of photon emission leading to the radiative decay of optical excitations.

The particles in the chain (Fig. 2) are coupled by electromagnetic interaction, leading to the formation of collective optical modes (polariton excitations) within the chain. Translational symmetry of the system with respect to its shift by lattice period a enables us to classify these collective excitations by their quasi-wave vectors k, which belong to the interval $(-\pi/a, \pi/a)$ and are characterized by dispersion law $\omega(k)$. Generally these modes can be lossy because they can emit photons in the transverse direction (Fig. 2). Characteristic photon wave vector q is defined by excitation frequency ω_0 through the vacuum dispersion relation

$$q = \frac{\omega(k)}{c} \approx \frac{\omega_0}{c}. \tag{1}$$

As was discussed above, we have neglected polariton dispersion, assuming that electromagnetic coupling of resonant particles is much smaller than the particles' resonant frequency.

The photon formed as a result of decay of the excitation of the medium with wave vector k should have its projection to the chain axis (z direction) equal to k or different from k by an integer number of chain quanta $2\pi/a$. This requirement cannot be satisfied when excitation wave vector k exceeds photon wave vector q in relation (1). Because the absolute value of k is smaller than π/a, nondecaying excitations can exist in the wave-vector range

$(-\pi/a, -q)$, $(q, \pi/a)$ when photon wave vector q [relation (1)] is less than π/a. This is equivalent to the requirement that the lattice period be smaller than half of the resonant wavelength:

$$a < \frac{\lambda}{2} = \frac{\pi c}{\omega_0}. \tag{2}$$

Similar arguments were proposed by Afanas'ef and Kagan[30] to describe excitations in an array of Mössbauer nuclei.

Generally, one can find maximum quasi-momentum by considering the elementary cell of the inverted lattice, demonstrated in Fig. 3A for the linear chain of particles. The elementary cell of the inverted lattice occupies the segment from $(-\pi/a, \pi/a)$, and the maximum vector of the quasi-momentum goes from the origin to the right or the left end of the segment.

Our arguments can easily be extended to a planar layer of particles with interparticle distance a. For the practically important closely packed hexagonal lattice with interparticle distance a there is the weaker restriction (see Fig. 3B)

$$a < \frac{\lambda}{\sqrt{3}}. \tag{3}$$

An interesting question arises for dielectric particles that are capable of supporting Mie resonances: How large should the dielectric constant of the material be to reach the conditions of inequalities (2) and (3) at reasonable wavelengths? We considered spherical particles of diameter d (Fig. 2). Inequalities (2) and (3) can be satisfied if the particle diameter is less than the required minimum interparticle distance $(d < a)$. We have used the wavelengths of the first and second Mie resonances to test the minimum dielectric constant needed to satisfy requirements (2) and (3). Our estimates are not sensitive to the optical wavelength because of the scale invariance of Maxwell equations to changes of a wavelength and particle size by the same factor.

For the first (broad) Mie resonance we have the following requirements for one and two dimensions:

$$\epsilon^1_{1\text{-D}} > 3.8, \qquad \epsilon^1_{2\text{-D}} > 3.1, \tag{4}$$

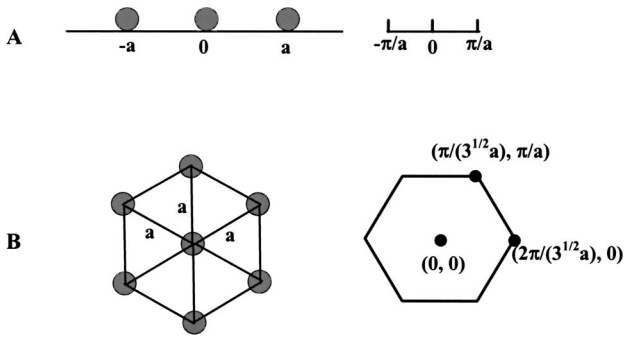

Fig. 3. Light-cone constraint in A, a linear 1-D chain of scattering particles and B, a 2-D closely packed lattice of scattering particles. The original lattice is shown at the right, and the inverse lattice is shown at the left. The maximum wave vector is π/a for one dimension and $2\pi/(3^{1/2}a)$ for two dimensions.

respectively. Note that, because the first Mie resonance is relatively broad, estimates (4) are crude. They can easily be satisfied for many dielectric materials of interest, including ZnO ($\epsilon \sim 5$), which is most often used in random lasers.[12,29]

For the second (much narrower) Mie resonance the light-cone constraint can be satisfied when

$$\epsilon^2_{1\text{-D}} > 7.5, \qquad \epsilon^2_{2\text{-D}} > 5.4, \tag{5}$$

for 1-D and 2-D chains, respectively. These requirements are stronger than inequalities (4), but they can still be satisfied for several materials including TiO_2, which has refractive index $n = \epsilon^{1/2}$, where $\epsilon^{1/2}$ is 2.6–2.9 (the upper limit is good for both 1-D and 2-D structures), lead oxides, GaAs, and some other compounds.

Our analysis of collective modes is more justified for the second Mie resonance than for the first, because its narrowness justifies its separate consideration. In contrast, the width of the first Mie resonance is comparable with the distance to the next resonance for the lowest dielectric constants permitted by inequalities (4).

Although our estimates [inequalities (4) and (5)] are crude, we hope that they have 10–20% accuracy based on the ratio of Mie resonance width to its frequency. Recent numerical comparisons of the coupled dipolar approach and exact modeling[8,32] also support the approximate relevance of the coupled dipolar approach under conditions of interest when the interparticle distance and the particle size are similar.

When inequalities (2) and (3) are satisfied one would expect that certain modes would possess high quality even in a finite-sized regular open system. We investigate these modes in Sections 3 and 4.

3. ONE-DIMENSIONAL CHAIN MODES: ANALYTICAL TREATMENT

We study optical modes within the framework of the coupled-dipole approach used, e.g., in Ref. 6. In this approach we replace each scattering particle by a resonant point dipole interacting with other dipoles, ignoring higher multipoles. This requires the particle size to be much smaller than the wavelength, a condition that can easily be satisfied for metal particles[6,7] but is more difficult for dielectrics.[28] We believe, however, that our approach should be valid at least qualitatively because the light-cone constraints in inequalities (2) and (3) cannot be sensitive to the number of multipoles under consideration. The dynamics of interacting dipoles in the frequency (z) domain, located within an infinite chain, can be approached by the following equation for local polarizations $\mathbf{p}_i$ (Ref. 6):

$$p_{i\alpha} = \sum_{\beta} \chi_{\alpha\beta}(z)\left(\mathbf{E}_{0i\beta} + \sum_{j\neq i,\gamma} V_{ij}{}^{\beta\gamma}\mathbf{p}_{j\gamma}\right), \tag{6}$$

where $\mathbf{E}_{0i}$ is the external electromagnetic field of frequency z taken at the position of dipole i, $\chi(z)$ is the local susceptibility at frequency z, and the second term in parentheses on the right-hand side represents the field of other dipoles. Greek subscripts α, β, and γ represent Cartesian coordinates x, y, and z, respectively, and i and j

represent the particles in the infinite chain, which range from $-\infty$ to $+\infty$. Interaction matrix V has the standard form of a retarded point dipole field (see, e.g., Refs. 6 and 28):

$$V_{ij}^{\alpha\beta} = \frac{\exp(iqr)}{r}\left[q^2(\delta_{\alpha\beta} - n_\alpha n_\beta) - \frac{\delta_{\alpha\beta} - 3n_\alpha n_\beta}{r^2} \times (1 - iqr)\right], \qquad q = \frac{z}{c}, \quad \mathbf{n} = \frac{\mathbf{r}}{r}. \tag{7}$$

Here we introduce wave vector q, expressed through field frequency z by use of the dispersion relation.

As was discussed in Section 1, we are interested in near-resonant conditions for the particles in the chain. We are able to approximate the susceptibility by a generalized Lorentzian shape

$$\chi_{\alpha\beta}(z) = \frac{\delta_{\alpha\beta} 2\omega_0 \mu^2}{\omega_0^2 - z^2 - 2iz\gamma}, \qquad \gamma = \frac{2}{3}\mu^2 q^3. \tag{8}$$

The notation is introduced to mimic the characteristic behavior of interacting electronic excitations. Parameter μ^2 is defined to make the problem similar to the problem of dipolar exciton transport. In fact it coincides (within Planck's constant $\mu^2 \to \mu^2/\hbar$) with the squared dipole moment of the degenerate atomic transition.[28]

The imaginary part in the denominator of the resonance susceptibility is caused by radiative losses that are due to the emission of photons. We ignored nonradiative processes for the dielectric materials under consideration.[28,29] We also assumed an isotropic susceptibility [Eq. (8)] that is due to the symmetry of the scattering spheres. Then we can rewrite Eq. (6) in the form of interacting dipolar oscillators[28]:

$$\left(-z^2 + \omega_0^2 - i\frac{4}{3}\omega_0\mu^2 q^3\right) p_{i\alpha} = \mu^2\left(E_{0i\alpha} + \sum_{j\neq i,\gamma} V_{ij}^{\alpha\gamma} p_{j\gamma}\right). \tag{9}$$

This form is convenient for further analytical and numerical investigations.

We are interested in the eigenmodes of the array of interacting dipoles that exist in the absence of external field $\mathbf{E}_0$. Generally these modes are lossy because of the finite probability that they will emit photons out of the chain (see Fig. 2), and therefore the imaginary part of z can be finite. At zero electric field the homogeneous problem [Eq. (9)] can be solved by Fourier transformation with wave vector $\mathbf{k}$ over the particle coordinates. All modes decouple into two transverse branches and one longitudinal branch. Below, we use the terms "transverse and longitudinal modes" in relation to the polarization orientation with respect to the chain or planar layer. If the polarization is perpendicular to the chain (or plane) where the particles are located we define this mode as the transverse mode. Otherwise the mode is longitudinal. Both polariton modes are composed of the superposition of longitudinal (closer than the wavelength) and transverse (wave zone) electromagnetic fields. The relative weight of longitudinal components increases with decreasing interparticle distance a.

The dispersion relationships take the form (cf. Ref. 6)

$$z^2 = \omega_0^2 + i\frac{4}{3}\omega_0\mu^2 q^3 - 2\omega_0\mu^2\left[\frac{q^2}{a} f_1(k, q) + \frac{iq}{a^2} f_2(k, q) - \frac{1}{a^3} f_3(k, q)\right],$$

$$f_p(k, q) = \sum_{n\neq 0} \frac{\exp[i(|n|qa - nka)]}{n^p} \tag{10}$$

for transverse modes and

$$z^2 = \omega_0^2 + i\frac{4}{3}\omega_0\mu^2 q^3 + 2\omega_0\mu^2\left[\frac{iq}{a^2} f_2(k, q) - \frac{1}{a^3} f_3(k, q)\right] \tag{11}$$

for longitudinal modes. Function f_1 can be evaluated analytically. When $0 < k < \pi/a$ (the opposite case, $-\pi/a < k < 0$, is similar) the function reads as

$$f_1(k, q) = 2\ln|\cos(ka) - \cos(qa)| - iqa + i\pi\sum_{n=0}^{\infty}\{\theta(-ka + qa - 2\pi n) + \theta[ka + qa - 2\pi(n + 1)]\}. \tag{12}$$

The logarithmic singularities in f_1 at $k = \pm q$ are due to the long-range [$1/r$, Eq. (7)] radiative coupling of interacting dipoles. The imaginary part of the sum increases by discrete jumps of $i\pi$ with increasing wave vector q (decreasing wave length $\lambda = 2\pi/q$) each time the argument of the logarithm crosses zero.

To evaluate the expressions for f_2 and f_3 one should integrate the result [Eq. (12)] over wave vector q from 0 to its actual value one or two times. The result cannot be expressed in terms of elementary functions for the real part, but the imaginary part can be evaluated explicitly (cf. Ref. 6). After straightforward integration one can evaluate the imaginary part of the squared frequency as

$$\mathrm{Im}\, z^2 = \pi\frac{\omega_0\mu^2 q^2}{a}\sum_{n=0}^{\infty}\left(\theta(-ka + qa - 2\pi n) \times\left[1 + \frac{(k + 2\pi n/a)^2}{q^2}\right] + \theta[ka + qa - 2\pi(n + 1)] \times\left\{1 + \frac{[-k + 2\pi(n + 1)/a]^2}{q^2}\right\}\right) \tag{13}$$

for transverse modes and

$$\mathrm{Im}\, z^2 = \pi \frac{\omega_0 \mu^2 q^2}{a} \sum_{n=0}^{\infty} \left(\theta(-ka + qa - 2\pi n) \times \left[1 - \frac{(k + 2\pi n/a)^2}{q^2} \right] + \theta[ka + qa - 2\pi(n+1)] \times \left\{ 1 - \frac{[-k + 2\pi(n+1)/a]^2}{2q^2} \right\} \right) \quad (14)$$

for longitudinal modes. In agreement with the light-cone constraint for the 1-D chain [inequality (2)] we can see that when the wavelength is sufficiently long ($qa < \pi$) the mode with wave vector k in the range $(q, \pi/a)$ has a zero decay rate. As we discussed in Section 2, these modes cannot decay radiatively because this process cannot occur with simultaneous conservation of energy and momentum.

Lasing from the chain is defined by the mode with the highest quality factor (smallest decay rate).[25,27] One can find this mode by minimizing the decay rates [Eqs. (13) and (14)] with respect to wave vector k in the range $(0, \pi/a)$ at fixed resonant photon wave vector q (frequency, $z = cq$). This minimization leads to different results for transverse and longitudinal modes. The decay rate of transverse modes changes discontinuously, possibly as a result of singularities in the spectrum [Eq. (12)] that are therefore absent in the longitudinal case. It reaches a minimum at $k = \pi/a$ for $\pi 2n < qa < \pi(2n + 1)$ and at $k = 0$, when $\pi(2n + 1) < qa < \pi(2n + 2)$ for any integer $n = 0, 1, 2, \ldots$. The general expression for the minimum decay rate for the transverse mode ($\mathrm{Im}\, z$) can be written as

$$\mathrm{Im}\, z = 2\pi \frac{n\mu^2 q^2}{a} \left[1 + \frac{(2n-1)(2n+1)}{3} \left(\frac{\pi}{aq} \right)^2 \right], \quad 2\pi n < qa < (2n+1)\pi,$$

$$\mathrm{Im}\, z = \pi \frac{\mu^2 q^2}{a} \times \left[1 + 2n + \frac{2n(n+1)(2n+1)}{3} \left(\frac{\pi}{aq} \right)^2 \right], \quad (2n+1)\pi n < qa < 2\pi n. \quad (15)$$

The dependence of relative decay rate $\mathrm{Im}(z)/\gamma$ on the ratio of the lattice period to the resonant wavelength, $a/\lambda = qa/(2\pi)$, is shown in Fig. 4 for transverse modes. It shows discontinuous nonmonotonic behavior as a result of logarithmic divergences in the spectrum [Eq. (12)].

For a longitudinal mode the analysis is easier because the decay rate is a decreasing, continuous function of wave vector k. Its minimum is always reached at a maximum of $k = \pi/a$. Thus we find that

$$\mathrm{Im}\, z = 2\pi \frac{n\mu^2 q^2}{a} \left[1 - \frac{(2n-1)(2n+1)}{3} \left(\frac{\pi}{aq} \right)^2 \right], \quad (2n-1)\pi < qa < (2n+1)\pi. \quad (16)$$

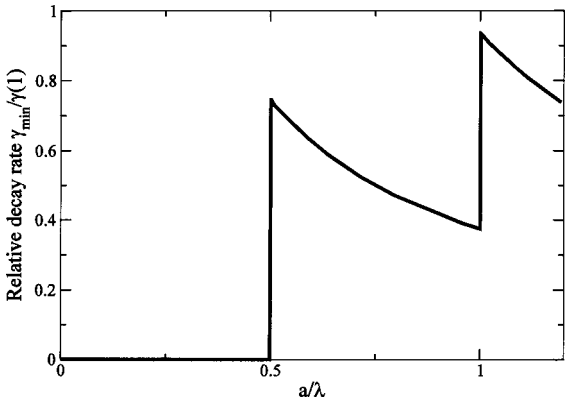

Fig. 4. Relative decay rate for the transverse mode of highest quality for wavelengths a/λ.

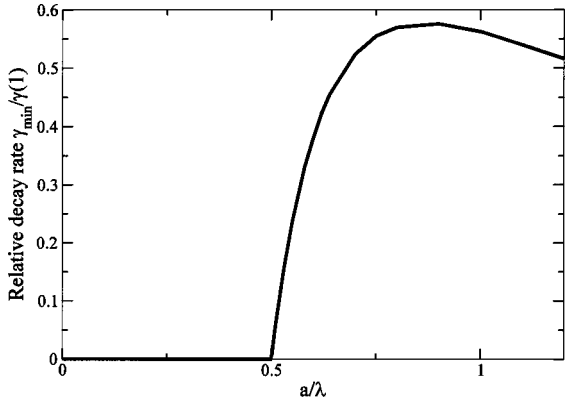

Fig. 5. Relative decay rate for the longitudinal mode of an infinite linear array of highest quality for wavelengths a/λ [$\gamma(1)$ is the single-particle decay rate].

The actual minimum of Eqs. (15) and (16) corresponds to the longitudinal mode described by Eq. (16). Both branches have zero minimum decay rates (infinite quality) when $(q < \pi/a)$. The dependence of relative decay rate $\mathrm{Im}(z)/\gamma$ on the ratio of the lattice period to the resonant wavelength $a/\lambda = qa/(2\pi)$ is shown in Fig. 5 for longitudinal modes. It is continuous because of the absence of the logarithmically diverging term in the spectrum [Eq. (11)] but is still nonmonotonic.

The finite chain of $N \gg 1$ particles that satisfy condition (2) should have large but finite quality. It is interesting to estimate the characteristic dependence of the decay rate on system size $L = Na$. We cannot solve the problem analytically because of the long-range character of dipolar coupling [Eq. (7)]. Instead, we model the system by a finite chain of N sites with the sites at the edges that have the decay rate $\gamma_m \sim \mu^2 q^3$ and nearest-neighboring coupling $V_m \sim \mu^2/a^3$. The finite decay rate arises from the presence of the edges. Therefore the oversimplified problem that we are going to consider can belong to the same universality class as the problem of interest. The amplitude for excitation at a certain site k ($0 \leqslant k \leqslant N$) should obey the equation (the rotating wave transformation is assumed to remove oscillations with a common frequency ω_0)

$$z f_i = -V_m[f_{i-1}(1 - \delta_{i1}) + f_{i+1}(1 - \delta_{iN})] - i\gamma_m f_i(\delta_{i1} + \delta_{iN}). \quad (17)$$

This equation leads to a standard dispersion law:

$$z = -2V_m \cos(ka), \tag{18}$$

where k is the wave vector and a is the chain period. In the finite chain the appropriate values of z and k can be found from the boundary conditions that follow from Eq. (17) at $i = 1$ or $i = N$. For the symmetric solutions with the highest quality we get the equation for the wave vector:

$$\frac{-2V_m \cos(ka) + i\gamma_m}{V_m} = -\frac{\cos[ka(N/2 - 1)]}{\cos(kaN/2)}. \tag{19}$$

The solutions with the smallest group velocity near the top and the bottom of band $k \sim 0$, $z \sim -2V_m$ or $k \sim \pi/a$, $z \sim 2V_m$, respectively, have longest lifetimes. Expanding the arguments of the cosine functions with respect to the small parameter ka or $\pi - ka \sim 1/L$, one can find the approximate solutions for modes closest to the edges of the band:

$$k_1 \approx \frac{\pi}{L} - \frac{\pi a}{L^2}\frac{1 + i\gamma_m/V_m}{1 + (\gamma_m/V_m)^2},$$

$$k_2 \approx \frac{\pi}{a} - \frac{\pi a}{L} - \frac{\pi}{L^2}\frac{1 + i\gamma_m/V_m}{1 + (\gamma_m/V_m)^2}. \tag{20}$$

One can find the decay rate of the corresponding modes by making use of dispersion relation (18), which yields

$$\mathrm{Im}\, z \approx 2\pi^2 V_m \left(\frac{a}{L}\right)^3 \frac{i\gamma_m V_m}{V_m^2 + \gamma_m^2}. \tag{21}$$

Thus our analysis predicts that in the finite system the decay rate of the most slowly decaying modes decreases with system size as $1/L^3$ when the light-cone conditions of inequalities (2) and (3) are satisfied. One can show that similar behavior is expected in a 2-D system. Our numerical study reported in Section 4 below seems to support this expectation.

It is interesting that in the limiting case $a \ll \lambda \ll L$ the decay rate is universal and does not depend on the small length scales. The qualitative behavior of the decay rate can be expressed by use of the definitions $V \sim \mu^2/a^3$ and $\gamma \sim \mu^2 q^3$ as

$$\mathrm{Im}\, z \approx \mu^2/L^3. \tag{22}$$

It is not clear, however, whether this expectation survives in the case of realistic interactions [Eq. (9)], including the long-range retarded interaction. Our numerical studies (see Section 4 below) do not fully support this conclusion.

Note that for interacting dipoles the relevant mode that has the smallest group velocity corresponds to the top of band $k \approx \pi/a$, whereas the modes near the bottom of band $k \sim 0$ are lossy.

A size dependence of the decay rate of the highest-quality mode $\gamma(L) \sim 1/L^3$ is also expected if we have a 3-D photonic crystal with a completely or incompletely forbidden band owing to a minimum in the group velocity in certain directions. This problem can be crudely modeled by the wave equation with the step-function potential $U > 0$ introduced between $x = 0$ and $x = L$ in the infinite system:

$$\left[-\frac{\mathrm{d}^2}{\mathrm{d}x^2} + U\theta(L - x)\theta(x)\right]\psi(x) = E\psi. \tag{23}$$

One can show that for a quasi-stationary solution with a real part of the energy closest to potential U, the imaginary part behaves as

$$\mathrm{Im}\, E \approx 4/\sqrt{U}L^3. \tag{24}$$

Similar behavior can be deduced from an analysis of the modes near the edge of the forbidden band performed in Ref. 18.

4. EFFECT OF FINITE SIZE AND DISORDERING ON MODE QUALITY: NUMERICAL APPROACH

To study the lasing thresholds under more-general conditions, we apply the numerical method developed previously.[28] The array of scattering particles is treated in the coupled-dipole approach [Eqs. (6)–(9) of Ref. 6]. This approach is relevant when the refractive index of the particles is much greater than 1. It also requires that $\lambda \gg d$, where d is the particle size (Fig. 2). Then the higher multipoles can be neglected. The dipole approach should be quite accurate for GaAs particles, which have a large refractive index, $n \approx 3.7$. It can also be justified for the plasmon resonances in metal particles.[10,11] We believe that it will be valid qualitatively for other systems (for instance, for ZnO and TiO_2 particle arrays) because the light-cone constraints of inequalities (2) and (3) are not sensitive to the number of multipoles that are taken into account.

As in Ref. 28, we have studied the value of the gain that should be added to the system to reach lasing instability for at least one mode. The gain can be introduced as an imaginary positive correction ig to the eigenfrequency of the oscillators on the left-hand side of Eq. (9). It describes stimulated emission inside the particles, caused by external optical pumping. This increase in the gain reduces the decay rates for the modes. When the first nondecaying mode appears, the system transitions into a lasing instability.[27,28] The algorithm with which to find that mode is organized as follows: The problem [Eq. (9)] can be written in matrix form:

$$(z + ig)^2\mathbf{P} = A(z)\mathbf{P}, \tag{25}$$

where $\mathbf{P}$ is a multicomponent vector that describes the polarizations of all dipoles and $A(z)$ is the interaction matrix that is frequency dependent. In the first step we select a random initial real frequency z (close to the average frequency ω_0), take the gain equal to zero, and diagonalize matrix A. Diagonalization leads to the sequence of eigenmodes $z_a = \omega_a - i\gamma_a$, $a = 1,\ldots N$. Then eigenmode b that has the minimum decay rate for all N modes is chosen. For the next step we choose $z = \omega_b$ and $g = \gamma_b$ and repeat the procedure described above approximately 10 times. This process converges exponentially to the mode $z = \omega^* - i\gamma^*$ that does not decay when gain g is equal to γ^*. Other methods have been used for relatively small systems to verify that this algorithm con-

verges to the true minimum. We believe that our approach for g gives a reasonable estimate of the mode decay rates without gain.

We used the Matlab software to perform the matrix diagonalization. It restricts our consideration to fewer than 2000 particles; above $N = 2000$, diagonalization takes an unacceptably long time. Also, the standard numerical diagonalization algorithms are expected to fail above $N = 5000$ because of divergences.[33] Special algorithms for large sparse matrices[31] are not helpful in our case because interaction (7) is long ranged, which makes matrix A in Eq. (25) strongly off diagonal. The interaction constants of the oscillators {dipolar matrix elements μ; Ref. 28 [Eq. (10)]} were taken sufficiently small to make the width of each scattering resonance much smaller than resonant frequency ω_0. In this limit the dependence of the lasing threshold on geometry (number of particles and their positions) is universal and is insensitive to frequency ω_0. This condition requires the width of the Mie resonances to be narrow compared with the light's frequency; this is true near light-cone constraint conditions (2) and (3) for sufficiently large particle dielectric constants (4) and (5).

We have considered finite linear and planar arrays of N particles. One generates the linear chain (Fig. 2) by placing N dipoles at equal distances a. The system size is accordingly $L = Na$. The planar layer is a closely packed hexagonal lattice with interatomic distance a. The specific radius $R \sim L$ has been chosen, and the circle of radius R has been filled by a hexagonal lattice of dipoles separated by distance a.

The dipole moment orientation for the particles can be taken either parallel or perpendicular to the array of the particles (linear or planar) to form longitudinal or transverse modes, respectively. In the regime of interest, when the collective modes with the very small decay rate $g \ll \gamma = (4/3)\mu^2 q^3$ are formed, the results are not qualitatively sensitive to our choice. In the 2-D case they are not sensitive in any regime. Therefore we restrict our consideration to transverse modes in a 1-D chain, where the discontinuity of the mode quality should show up at short wavelengths [Eqs. (15) and Fig. 4] and longitudinal modes in a 2-D planar layer, where the discontinuity occurs for all modes.

We begin with fully ordered finite systems. The criteria [inequalities (2) and (3)] for the qualitative changes in the lasing threshold behavior with wavelength were tested for a regular chain of $N = 500$ particles and a planar layer of $N = 1002$ particles. The computed dependence of the relative lasing threshold (the ratio of the best mode decay rate for an N-particle array to that for a single particle) on dimensionless ratio a/λ is shown in Fig. 6. In the 1-D case the decay rate drops by 6 orders of magnitude when interparticle distance a gets below $\lambda/2$, in agreement with the light-cone condition of inequality (2). In the 2-D case a sharp decrease in the lasing threshold (3 orders of magnitude) takes place when $a < 0.58\lambda \approx \lambda/3^{1/2}$, in perfect agreement with the criterion [inequality (3)] for the hexagonal lattice. The overall effect is much stronger in the 1-D case, which agrees qualitatively with our expected $1/L^3$ dependence for the decay rate derived in Section 3 [relations (22) and (24)]. In terms of particle number, the expected dependence is $1/N^3$ in one dimension and $1/N^{3/2}$ in two dimensions. Accordingly, the number of orders of magnitude in the overall change for similar numbers of particles is twice as large in one as in two dimensions. The sharp change itself is not surprising for systems with large numbers N of particles, because for an infinitely long system the decay rate should vanish in the long-wavelength case [inequalities (2) and (3) and Eqs. (15) and (16)], whereas for short wavelengths it is close to the single-particle decay rate. The discontinuous change in the relative lasing threshold

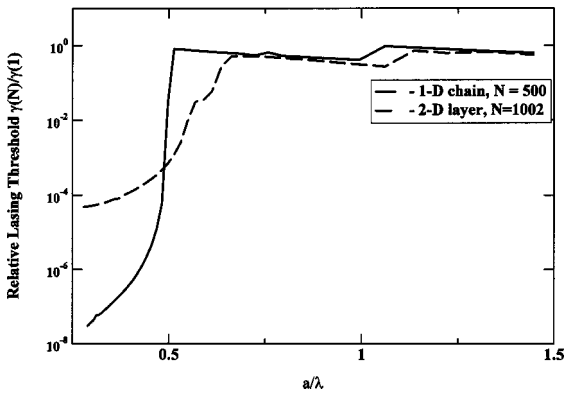

Fig. 6. Relative lasing threshold for finite chain and planar layers of resonant dipoles [$\gamma(1)$ is the single-particle decay rate].

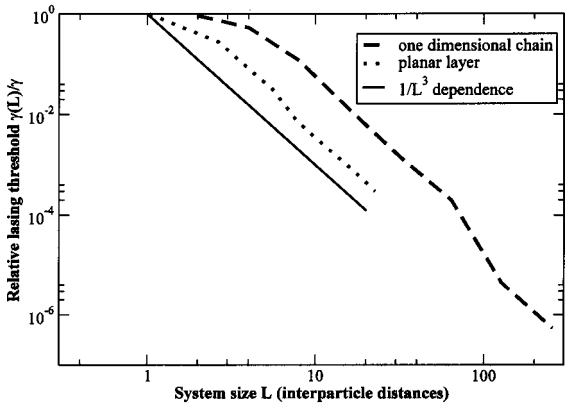

Fig. 7. Dependence of lasing threshold on length for finite chain and planar layers of resonant dipoles.

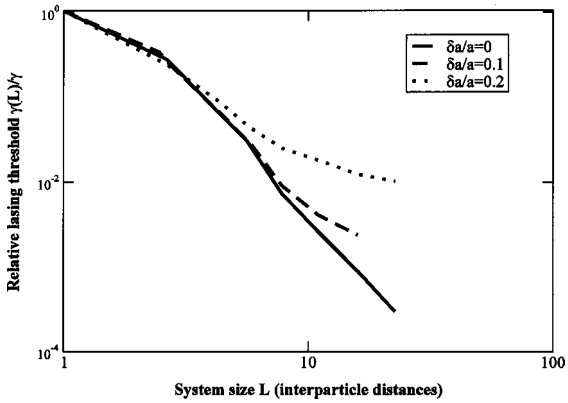

Fig. 8. Dependence of lasing threshold on site disorder for the planar layer (long wavelength, $a/\lambda = 0.45$).

(decay rate) in both one and two dimensions for short wavelengths (Fig. 6) agrees with the results of analytical derivations for the transverse modes in a 1-D chain [Fig. 4 and Eqs. (15)].

To examine the dependence of mode quality on system size we studied the lasing threshold at different system sizes (numbers of particles N; Fig. 7) for fixed interparticle distance a at long wavelength when the light-cone constraint is satisfied ($a/\lambda = 0.4$). The system size in the 2-D layers has been defined as the square root of the number of particles. The solid curve shows $1/L^3$ dependence [relation (22)] derived in Section 3. We can see that the numerical studies seem to support theoretical expectations.

It is generally difficult to make materials perfectly ordered. To address this issue we studied the effect of disordering on the lasing threshold. Three possible effects were examined, including fluctuations in interparticle distance a (shown in Figs. 8 and 9), dipole moment directions, and resonant frequencies ω_0 (which can be used to describe the effect of particle size fluctuation on Mie resonances). In all cases disordering was generated as random Gaussian noise with a certain standard deviation (indicated as δa in Figs. 8–10 for an interparticle distance fluctuation). The lasing threshold shown there was averaged over several hundred particle configurations with a fixed amount of disorder. We took the interparticle distance close to the threshold value in both cases, $a = 0.4\lambda$ for long wavelengths (two dimensions at Fig. 8 and one dimension at Fig. 9) and $a = 0.53\lambda$ for short wavelengths in one dimension (Fig. 10). Probes of other particle densities within the range $0.25\lambda < a < 0.5\lambda$ showed qualitative universality of the lasing threshold behavior at $a > \lambda/2$ and $a < \lambda/2$ such that Figs. 8 and 9 represent appropriately the qualitative effect of randomness.

For long wavelength (Figs. 8 and 9) the general tendency can be summarized as follows: Until some finite size L_c (number of particles N_c) defined by disordering is achieved, the threshold follows the regular system behavior $g(L) \sim L^{-3}$. At larger sizes it decreases more slowly. Analysis of the lasing mode's spatial profile and size (in terms of the participation ratio) shows that at system size $L < L_c$ ($L_c \sim 20a$ for 20% disordering, $L_c = \infty$ for the regular system) the size of the mode is comparable to the size of the system. At larger system size $L > L_c$ the size

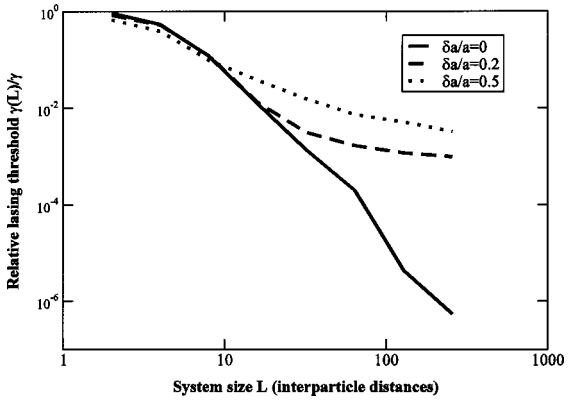

Fig. 9. Dependence of lasing threshold on site disorder for the 1-D chain (long wavelength, $a/\lambda = 0.4$).

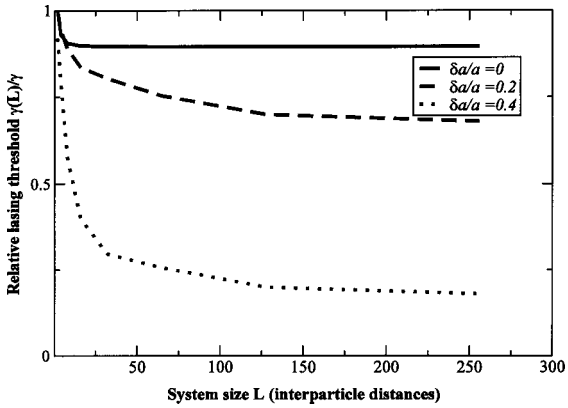

Fig. 10. Dependence of lasing threshold on site disorder for the 1-D chain (short wavelength, $a/\lambda = 0.53$).

of the lasing mode stays near scale L_c, and further change in the lasing threshold is due to fluctuations in achievement of the most efficient mode, discussed in Ref. 28. In the limit of full disordering in the interparticle distances and dipole directions (no frequency disordering), dependence $g(N) \sim N^{-1/2}$ found in Ref. 28 has been reproduced.

For short wavelengths (Fig. 10), strong disordering leads to reduction of the lasing threshold for large arrays, unlike in the long-wavelength regime. This is the effect of fluctuations on a scale of several particles that forming critical configurations and possessing high optical quality.[28] The highest-quality modes always involve few (~5) particles. In full disordering, the decay rate of the best modes decreases with system size also according to the law close to $g(N) \sim N^{-1/2}$ found in Ref. 28. One should note the $N^{-1/2}$ dependence for both one and two dimensions.

5. DISCUSSION AND CONCLUSIONS

We have shown that, when the light-cone constraint is satisfied, high-quality modes can be obtained in low-dimensional arrays of resonant particles. The quality factor of the mode increases as the cube of the system size when the interparticle distance is smaller than half of the resonant wavelength in one dimension and is 0.58 of it in a two-dimensional closely packed hexagonal array. This happens in spite of the open character of the system, which suggests strong coupling to the vacuum radiation (Fig. 2). An array of a few tens of identical particles with dispersion in the interparticle distance as large as 20% possesses an optical quality nearly 1000 times higher than that for a single particle (Fig. 9). Assuming a particle diameter and an interparticle distance of ~100 nm, one can make the lasing cavity of the size as small as 1 μm and obtain the result suggested in Ref. 13.

In principle, a chain or planar lattice array structure may not be the optimum structure. Reference 31 describes a V-shaped regular array of silver particles that represents two chains with one common end. The particles have a diameter of ~10 nm, which is much smaller than the resonant wavelength. Therefore the light-cone constraint is perfectly satisfied for that system. The authors of Ref. 31 describe several modes with extremely

small radiative decay rates. They identify these nonradiative surface plasmon modes as dark modes. We believe that the extremely high quality of these modes could have an origin similar to that of the modes described here (destructive interference of dipolar emission forming guided modes) but with greater efficiency than those in the linear chain. Possibly the placement of particles in a circular boundary can also be efficient because of the presence of long-living whispering-gallery modes (see Refs. 34 and 35 and the discussion below). The dark modes in the array of silver particles studied in Ref. 31 are not interesting for possible applications because of the strong absorption of energy by the conducting electrons. Optical pumping of similar dark modes in dielectric arrays can lead to much higher energy concentration, stimulated emission, lasing, and other effects of interest. Experimentally these modes should be excited by higher-energy pumping of light through internal conversion rather than by direct pumping because of the weak coupling of these modes to the external electromagnetic field.

Thus the optical investigation of microscopic structures of a few tens of identical dielectric particles with a sufficiently large dielectric constant ordered in a regular 1-D or 2-D array has led to the discovery of high-quality modes that should manifest themselves in a wide variety of phenomena including lasing and coherent energy transport along the chain of particles.[36,37] We hope that our report will attract the attention of experimentalists to these fascinating systems.

It is also important from the practical point of view that the same increase in quality requires the use of many more particles in a 2-D system (N^2) than in a 1-D (N) system for arbitrary N. Therefore 1-D chains are more interesting than planar arrays for experimental study.

Another important message of this paper is the description of the $1/L^3$ behavior of the decay rates in several classes of structure, including regular 1-D and 2-D arrays with the light-cone constraints of inequalities (2) and (3) and in 3-D photonic crystals with completely and incompletely forbidden optical bands. Lasing from regular 3-D systems with an incompletely forbidden band has been studied in two experiments performed with liquid crystals by Kopp *et al.*[17] and in optical polymers by Shkunov *et al.*[16,20] These systems show bright lasing modes. It was shown in Refs. 16 and 20 that lasing in highly ordered structures is more efficient that in fully random materials. This result is not surprising, because the lasing threshold in a random material (in the absence of Anderson localization) shows the size dependence

$$g \sim v \frac{l_{\mathrm{tr}}}{L^2}, \tag{26}$$

where v is the group velocity of light inside the medium and l_{tr} is the transport length for light scattering by disordering.[26] As follows from the discussion in Section 3 [relation (24)], in the system with forbidden optical bands the lasing threshold scales as

$$g \sim C/L^3, \tag{27}$$

where C is a proportionality constant. In highly ordered systems relation (27) leads to a lower lasing threshold than relation (26) for a disordered medium. Finite disordering should lead to replacement of system size L in relation (27) by transport length l_{tr}. Then the lasing threshold should be expressed as

$$g \sim \min\left(v \frac{l_{\mathrm{tr}}}{L^2}, \frac{A}{{l_{\mathrm{tr}}}^2} \right). \tag{28}$$

In the regime of sufficiently strong disordering (smaller transport length) random lasing should dominate regular lasing, as was demonstrated in Ref. 16. As was expected theoretically, the lasing threshold is smaller in a highly ordered system than in a highly disordered one.[16] We do not apply the present theory to interpretation of experiment[16] in much detail here because the complicated relationship between the measured pump power needed to reach lasing and the gain rate requires special study.[38]

Consider the relation of our results to other studies of random lasing in different conditions, materials, and regimes. Table 1 summarizes our knowledge of the various length dependences predicted theoretically and used in attempting to interpret experimental data. It is clear that the $1/L^3$ dependence of the required gain rate on system size is highly efficient compared to other mechanisms excluding the regime of the strong localization of light. That regime is hard to attain, and therefore the practical achievement of the open structures suggested in this study can be much easier to design.

We should briefly mention other theoretical and experimental developments related to random lasing that are possibly outside the scope of our discussion above. A model of fluctuational whispering-gallery modes in open 2-D and closed 3-D structures was suggested in Refs. 34 and 35. The simplest example of the whispering gallery mode is a circular array of nanoparticles. We tested the decay rates in circular arrays of particles under the conditions of Fig. 7 in the scalar model approach [only the $\exp(iqr)/r$ term in Eq. (9)]. For as many as a few hun-

Table 1. Summary of Theoretical Predictions of Lasing Threshold Behavior in Various Situations

Property	Open Systems				Closed Systems	
Dimensionality	1-D		2-D		3-D	
Lattice period	$a < \lambda/2$	$a > \lambda/2$	$a < \lambda/3^{1/2}$	$a > \lambda/3^{1/2}$		
Order	L^{-3}	L^{0}	L^{-3}	L^{0}	L^{-3}	
					Localization	Delocalization
Disorder	$L^{-1/2}$		L^{-1}		$\exp(-L/1)$	L^{-2}

dreds of particles we did not see a qualitative deviation from the linear chain behavior (Fig. 7), whereas at large sizes, circular arrays seem to be more efficient. This result agrees with the analytical solution of the continuous scalar model of distributed dipolar density at the circle. This solution predicts a superexponential decrease of the mode decay rate with increasing numbers of particles (proportional increase of the circle radius), in qualitative agreement with expectations expressed in Ref. 35. Analysis in detail is beyond the scope of this paper.

We should also mention that our 2-D numerical simulations[28] do not produce the high-quality modes of circular shape predicted in Ref. 35. This might be so because we did not introduce the correlations required in Ref. 35. The analysis of Refs. 34 and 35 is applicable to 2-D electronic systems and 3-D optical systems. However, when one is considering applications to three dimensions the decay is limited by two factors: the long lifetime within the randomly formed toroidal cavity and the time needed for leaving the sample. When there are no correlations between disordering, the second time seems to dominate, leading to the dependence on diffusion law of the lasing threshold,[26] whereas correlations can make the effect of the whispering-gallery trapping much stronger.[35] The actual effect of fluctuations should be tested in advanced numerical simulations, with correlations taken into account.

Experimental analysis of random lasing based on Nd (Refs. 39 and 40) showed many special characteristics that in some aspects are similar to and in other aspects are different from those of nanopowder lasers.[12,14] These systems have different characteristic time and spectrum properties, so they might require a special analysis. It is clear that the use of rare-earth materials can lead to progress in reducing laser threshold remarkably, and thus make random lasers more attractive for practical applications.

ACKNOWLEDGMENTS

This research was supported by the U.S. Department of Defense Multidisciplinary University Research Initiative program, by the Materials Research Science and Engineering Centers/National Science Foundation (MRSEC/NSF) program through the Northwestern University MRSEC (grant DMR-00076797) and the NSF (grant DMR-0093949). H. Cao acknowledges support from the David and Lucile Packard Foundation.

A. L. Burin's e-mail address is aburin @tulane.edu.

REFERENCES

1. E. Yablonovitch, T. J. Gmitter, R. D. Meade, A. M. Rappe, K. D. Brommer, and J. D. Joannopoulous, "Donor and acceptor modes in photonic band-structure," Phys. Rev. Lett. **67**, 3380–3383 (1991).
2. D. F. Sievenpiper, M. E. Sickmiller, and E. Yablonovitch, "3D wire mesh photonic crystals," Phys. Rev. Lett. **76**, 2480–2483 (1996).
3. D. S. Wiersma, P. Bartolini, A. Lagendijk, and R. Righini, "Localization of light in a disordered medium," Nature **390**, 671–673 (1997).
4. A. A. Chabanov, M. Stoytchev, and A. Z. Genack, "Statistical signatures of photon localization," Nature **404**, 850–853 (2000).
5. E. J. Zeman and G. C. Schatz, "An accurate electromagnetic theory study of surface enhancement factors for Ag, Au, Cu, Li, Na, Al, Ga, In, Zn, and Cd," J. Phys. Chem. **91**, 634–643 (1987).
6. V. A. Markel, "Coupled-dipole approach to scattering of light from a one-dimensional periodic dipole structure," J. Mod. Opt. **40**, 2281–2291 (1993).
7. V. M. Shalaev and A. K. Sarychev, "Nonlinear optics of random metal–dielectric films," Phys. Rev. B **57**, 13,265–13,288 (1998).
8. K. L. Kelly, E. Coronado, L. L. Zhao, and G. C. Schatz, "The optical properties of metal nanoparticles: the influence of size, shape, and dielectric environment," J. Phys. Chem. B **107**, 668–677 (2003).
9. G. C. Schatz, "Electrodynamics of nonspherical noble metal nanoparticles and nanoparticle aggregates," J. Mol. Struct.: THEOCHEM **573**, 73–80 (2001).
10. A. K. Sarychev and V. M. Shalaev, "Theory of nonlinear optical responses in metal–dielectric composites," Top. Appl. Phys. **82**, 169–184 (2002).
11. M. I. Stockman, S. V. Faleev, and D. J. Bergman, "Coherent control of femtosecond energy localization in nanosystems," Phys. Rev. Lett. **88**, 067402 (2002).
12. H. Cao, Y. G. Zhao, S. T. Ho, E. W. Seelig, Q. H. Wang, and R. P. H. Chang, "Random laser action in semiconductor powder," Phys. Rev. Lett. **82**, 2278–2281 (1999).
13. D. Wiersma, "Laser physics—the smallest random laser," Nature **406**, 132–132 (2000).
14. S. V. Frolov, Z. V. Vardeny, A. A. Zakhidov, and R. H. Baughman, "Laser-like emission in opal photonic crystals," Opt. Commun. **162**, 241–246 (1999).
15. O. Toader and S. John, "Proposed square spiral microfabrication architecture for large three-dimensional photonic band gap crystals," Science **292**, 1133–1135 (2001).
16. M. N. Shkunov, Z. V. Vardeny, M. C. DeLong, R. C. Polson, A. A. Zakhidov, and R. H. Baughman, "Tunable, gap-state lasing in switchable directions for opal photonic crystals," Adv. Funct. Mater. **12**, 21–26 (2002).
17. V. I. Kopp, A. Z. Genack, and Z. Q. Zhang, "Large coherence area thin-film photonic stop-band lasers," Phys. Rev. Lett. **86**, 1753–1756 (2001).
18. J. M. Bendickson, J. P. Dowling, and M. Scalora, "Analytic expressions for the electromagnetic mode density in finite one-dimensional, photonic band-gap structures," Phys. Rev. E **53**, 4107–4121 (1996).
19. J. P. Dowling, M. Scalora, M. J. Bloemer, and C. M. Bowden, "The photonic band-edge laser—a new approach to gain enhancement," J. Appl. Phys. **75**, 1896–1899 (1994).
20. M. N. Shkunov, N. C. DeLong, M. E. Raikh, Z. V. Vardeny, A. A. Zakhidov, and R. H. Baughman, "Photonic versus random lasing in opal single crystals," Synth. Met. **116**, 485–491 (2001).
21. S. G. Johnson, S. Fan, P. R. Villeneuve, J. D. Joannopoulos, and L. A. Kolodziejski, "Guided modes in photonic crystal slabs," Phys. Rev. B **60**, 5751–5758 (1999).
22. S. G. Johnson, S. Fan, A. Mekis, and J. D. Joannopoulos, "Multipole-cancellation mechanism for high-Q cavities in the absence of a complete photonic band gap," Appl. Phys. Lett. **78**, 3388–3390 (2001).
23. S. Fan and J. D. Joannopolous, "Analysis of guided resonances in photonic crystal slabs," Phys. Rev. B **65**, 235112 (2002).
24. S. John, "Localization of light," Phys. Today **44**(5), 32–40 (1991).
25. A. L. Burin, M. A. Ratner, H. Cao, and S. H. Chang, "Random laser in one dimension," Phys. Rev. Lett. **88**, 093904 (2002).
26. V. S. Letokhov, "Generation of light by a scattering medium with negative resonance absorption," Sov. Phys. JETP **26**, 835–840 (1968).
27. T. S. Misirpashaev and C. W. J. Beenakker, "Lasing threshold and mode competition in chaotic cavities," Phys. Rev. A **57**, 2041–2045 (1998).

28. A. L. Burin, M. A. Ratner, H. Cao, and R. P. H. Chang, "Model for a random laser," Phys. Rev. Lett. **87**, 215503 (2001).
29. Y. Ling, H. Cao, A. L. Burin, M. A. Ratner, X. Liu, E. W. Seelig, and R. P. H. Chang, "Investigation of random lasers with resonant feedback," Phys. Rev. A **64**, 063808 (2001).
30. A. M. Afanas'ev and Yu. Kagan, "Change of resonance nuclear parameters during scattering by regular systems," Sov. Phys. JETP **23**, 178–184 (1966).
31. D. J. Bergman and M. I. Stockman, "Surface plasmon amplification by stimulated emission of radiation: quantum generation of coherent surface plasmons in nanosystems," Phys. Rev. Lett. **90**, 027402 (2003).
32. C. L. Haynes, A. D. McFarland, L. L. Zhao, R. P. Van Duyne, G. C. Schatz, L. Gunnarsson, J. Prikuli, B. Kasemo, and M. Käll, "Nanoparticle optics: the importance of radiative dipole coupling in two-dimensional nanoparticle arrays," J. Phys. Chem. B (to be published).
33. P. Sievert, Department of Physics and Astronomy, Northwestern University, Evanston, Illinois 60208-3113 (personal communication, 2003).
34. V. M. Apalkov, M. E. Raikh, and B. Shapiro, "Crossover between universality classes in the statistics of rare events in disordered conductors," Phys. Rev. Lett. **89**, 126601 (2002).
35. V. M. Apalkov, M. E. Raikh, and B. Shapiro, "Random resonators and prelocalized modes in disordered dielectric films," Phys. Rev. Lett. **89**, 016802 (2002).
36. M. L. Brongersma, J. M. Hartman, and H. A. Atwater, "Electromagnetic energy transfer and switching in nanoparticle chain arrays below the diffraction limit," Phys. Rev. B **62**, R16356 (2000).
37. S. A. Maier, M. L. Brongersma, and H. A. Atwater, "Electromagnetic energy transport along arrays of closely spaced metal rods as an analogue to plasmonic devices," Appl. Phys. Lett. **78**, 16–18 (2001).
38. A. L. Burin, M. A. Ratner, and H. Cao, "Understanding and control of random lasing," Physica B (to be published).
39. G. R. Williams, S. B. Bayram, S. C. Rand, T. Hinklin, and R. M. Laine, "Laser action in strongly scattering rare-earth-metal-doped dielectric nanophosphors," Phys. Rev. A **65**, 013807 (2002).
40. M. Bahoura, K. J. Morris, and M. A. Noginov, "Threshold and slope efficiency of $Nd_{0.5}La_{0.5}Al_3(BO_3)_4$ ceramic random laser: effect of the pumped spot size," Opt. Commun. **201**, 405–411 (2002).